

Central and Enteric Neuroprotective Effects by *Eucommia ulmoides* Extracts on Neurodegeneration in Rotenone-induced Parkinsonian Mouse

Fuminori Imafuku^a, Ikuko Miyazaki^a, Jin Sun^a, Sunao Kamimai^b,
Takashi Shimizu^b, Toshiaki Toyota^b, Yusei Okamoto^b, Nami Isooka^a,
Ryo Kikuoka^{a,c}, Yoshihisa Kitamura^{c,d}, and Masato Asanuma^{a*}

Department of Medical Neurobiology, ^aOkayama University Graduate School of Medicine, Dentistry and Pharmaceutical Sciences, ^bOkayama University Medical School, ^cDepartment of Pharmacy, Okayama University Hospital, Okayama 700-8558, Japan, ^dDepartment of Pharmacotherapy, School of Pharmacy, Shujitsu University, Okayama 703-8516, Japan

Parkinson's disease (PD) is a progressive neurodegenerative disease of both the central and peripheral / enteric nervous systems. Oxidative stress and neuroinflammation are associated with the pathogenesis of PD, suggesting that anti-oxidative and anti-inflammatory compounds could be neuroprotective agents for PD. *Eucommia ulmoides* (EU) is a traditional herbal medicine which exerts neuroprotective effects by anti-inflammatory and anti-oxidative properties. Our previous study showed that treatment with chlorogenic acid, a component of EU, protected against neurodegeneration in the central and enteric nervous systems in a PD model. In this study, we examined the effects of EU extract (EUE) administration on dopaminergic neurodegeneration, glial response and α -synuclein expression in the substantia nigra pars compacta (SNpc), and intestinal enteric neurodegeneration in low-dose rotenone-induced PD model mice. Daily oral administration of EUE ameliorated dopaminergic neurodegeneration and α -synuclein accumulation in the SNpc. EUE treatment inhibited rotenone-induced decreases in the number of total astrocytes and in those expressing the antioxidant molecule metallothionein. EUE also prevented rotenone-induced microglial activation. Furthermore, EUE treatment exerted protective effects against intestinal neuronal loss in the PD model. These results suggest that EU exerts neuroprotective effects in the central and enteric nervous systems of rotenone-induced parkinsonism mice, in part by glial modification.

Key words: *Eucommia ulmoides*, dopamine neuron, enteric neuron, glia, Parkinson's disease

Parkinson's disease (PD) is characterized by motor symptoms based on dopaminergic neuronal death in the substantia nigra pars compacta (SNpc). PD patients also exhibit non-motor symptoms, such as olfactory impairment, orthostatic hypotension and constipation, which precede motor symptoms by 10~20 years [1,2]. In Braak's staging theory, it is hypothesized that Lewy body, a hallmark of PD pathol-

ogy, composed by α -synuclein (α -Syn), emerges in the olfactory bulb and the dorsal motor nucleus of the vagus nerve and propagates to the SNpc and the cortex along with progression of PD [3]. Lewy body-like inclusions are also observed in the enteric plexus of PD patients [4,5]. As well as intracerebral inoculation, intestinal inoculation of α -Syn induced dopaminergic neurodegeneration in the SNpc and motor impairment, but this gut-to-brain transmission of α -Syn is prevented

Received November 15, 2021; accepted January 25, 2022.

*Corresponding author. Phone: +81-86-235-7096; Fax: +81-86-235-7103
E-mail: asachan@cc.okayama-u.ac.jp (M. Asanuma)

Conflict of Interest Disclosures: No potential conflict of interest relevant to this article was reported.

by vagotomy [6]. Therefore, PD pathology accompanied with Lewy bodies can originate in the enteric nervous system (ENS) and then ascend to the central nervous system (CNS) in a prion-like fashion [7-12].

Unlike familial PDs caused by genetic mutations, both genetic factors and environmental factors like pesticide and metal exposure are involved in the pathogenesis of sporadic PD. Exposure to the pesticide rotenone, which is a mitochondria complex I inhibitor, is known as an epidemiological risk factor for PD; indeed, rotenone is utilized to produce PD model animals [13, 14]. We recently reported that chronic exposure to low-dose rotenone reproduced neurodegeneration of both the nigrostriatal dopaminergic neurons and the peripheral enteric neurons to induce motor impairment and bowel dysfunction, respectively [15].

Oxidative stress and inflammatory reactions play pathological roles in the dopaminergic neurodegeneration of PD. Various studies have shown that dysfunction of astrocytes is also involved in the pathogenesis of PD [16, 17] and that astrocytes protect neurons by production and/or secretion of neurotrophic factors and anti-oxidative molecules, such as glutathione and metallothionein (MT) [18-20]. MT is a cysteine-rich metal-binding protein that regulates homeostasis of metals such as zinc and has strong anti-oxidative effects through its 20 cysteine residues [21]. The two abundant isoforms, MT-1 and MT-2, expressed ubiquitously in most organs, are released from astrocytes, and their depletion has been shown to aggravate rotenone-induced neurodegeneration in both the CNS and ENS [22, 23]. Our recent study showed that oral administrations of chlorogenic acid and caffeic acid of coffee components exerted neuroprotective effects on low-dose rotenone-induced dopaminergic neuronal loss in the SNpc and on the neurodegeneration of the myenteric plexus by up-regulating MT-1,2 in striatal astrocytes and enteric glial cells [24].

The cortex and leaves of *Eucommia ulmoides* (EU) are consumed as tea or herbal medicine in China and Japan, and contain many beneficial components of polyphenols and iridoids, such as chlorogenic acid and aucubin [25]. EU has anti-rheumatic effects and neuroprotective effects associated with its anti-oxidative and anti-inflammatory properties [26-28]. Chlorogenic acid, which was shown to protect against low-dose rotenone-induced neurodegeneration in the SN and the myenteric plexus [24], is a component of EU. In this

study, we examined the neuroprotective effect of *Eucommia ulmoides* extracts (EUE) against neurodegeneration and glial responses in the CNS and ENS of rotenone-treated PD model mice.

Materials and Methods

Animals and materials. All experimental procedures were conducted in accordance with the Policy on the Care and Use of Laboratory Animals, Okayama University, and were approved by the Animal Care and Use Committee, Okayama University (approved reference number: OKU-2019102). Male C57BL/6J mice at 7 weeks of age were purchased from Charles River Japan, Inc. (Yokohama, Japan). Mice were housed with a 12-h light/dark cycle at constant temperature (23°C) and given *ad libitum* access to food.

Extract from leaves of EU prepared as previously reported [29,30] was deposited at R&D Center, Kobayashi Pharmaceutical Co., Ltd. (Osaka, Japan). Powdered EUE contained geniposidic acid 58.98 mg/g, asperuloside 12.97 mg/g and chlorogenic acid 40.30 mg/g.

Rotenone-treated PD model mice and administration of EUE. Eight-week-old C57BL/6J mice underwent pre-assessment one week prior to the experiment. At 9 weeks of age, an osmotic mini pump (Alzet, #2004, DURECT Corporation, Cupertino, CA, USA) containing vehicle (mixture of equal volumes of dimethylsulfoxide and polyethyleneglycol) or rotenone (10.4 mg/ml, Sigma-Aldrich, St. Louis, MO, USA) dissolved in the vehicle was implanted under the skin on the back of each mouse, which had been anesthetized by isoflurane inhalation. Using implanted osmotic mini pump, mice were subcutaneously injected with rotenone (2.5 mg/kg/day) or vehicle for 4 weeks. Daily oral administration of EUE (600 mg/kg/day) dissolved in water was started at 1 week prior to the implantation of rotenone-filled pumps, and then continued 5 days/week during the rotenone treatment (Fig. 1A). The EUE concentration was decided based on a previous report [27].

Body weight measurement and behavioral assessment. Body weight was measured, and behavioral assessment was performed at 1 week before implantation of the pump (pre; 8 weeks old), on the day of implantation (0; at 9 weeks old), and at 1 day and 1, 2, 3 or 4 weeks after implantation of the vehicle- or rote-

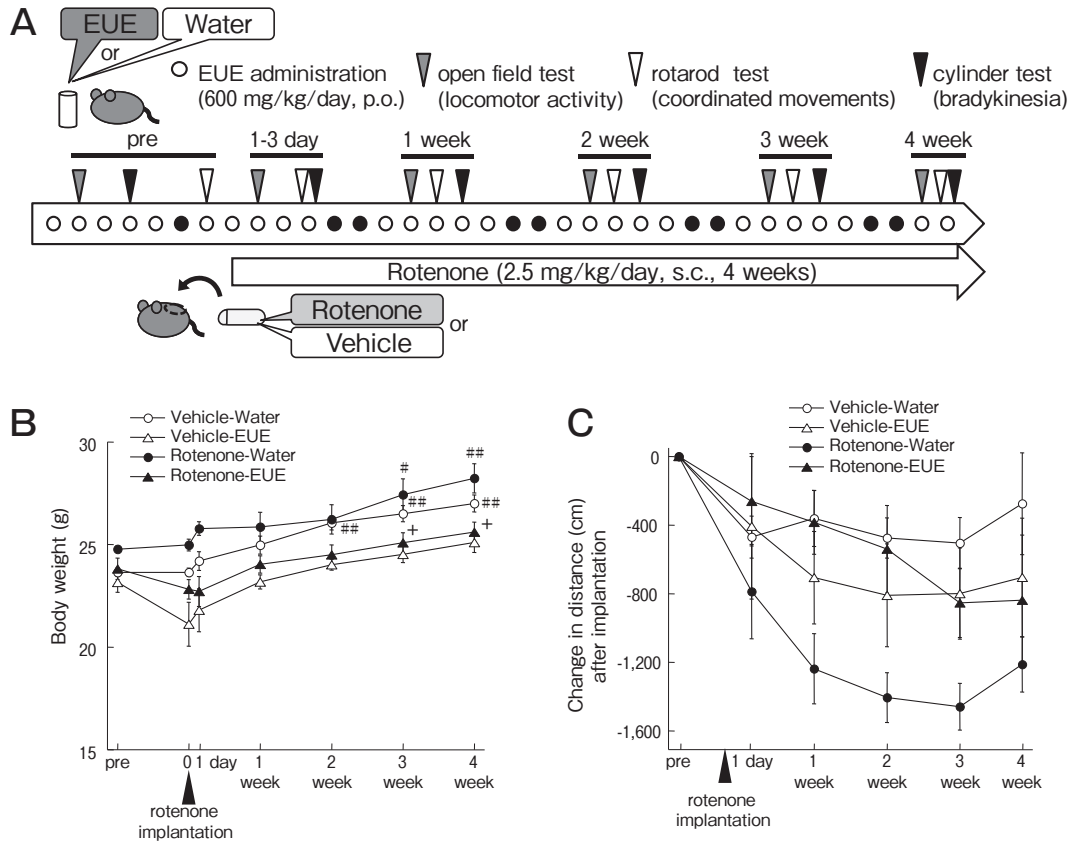


Fig. 1 EUE administration and rotenone-treated PD model mice. **A**, Schematic illustration of the administration schedule. An osmotic mini pump filled with rotenone or vehicle was implanted under the back skin of male C57BL/6J mice and was used for subcutaneous infusion of rotenone (2.5 mg/kg/day) or vehicle for 4 weeks (Vehicle-Water group: n=4, Vehicle-EUE group: n=5, Rotenone-Water group: n=4, Rotenone-EUE group: n=6). EUE (600 mg/kg/day) or vehicle was orally administered to mice 5 days/week for 5 weeks from 1 week prior to the implantation of osmotic pump. An open field test was performed 1 week before rotenone implantation (pre) and at 1 day, and 1, 2, 3 and 4 weeks after the implantation of the rotenone-filled osmotic pump; **B & C**, Effects of EUE administration on body weight changes (**B**) and locomotor activity assessed by the open field test (**C**) in rotenone-treated PD model mice. Each value represents the mean \pm SEM (n=4-6). Changes after implantation of rotenone pumps are indicated by the following symbols: * p <0.05; ** p <0.01 vs. pre-implantation of pump; + p <0.05 vs. Rotenone-Water group.

none-filled pump (Fig.1A). Evaluations were performed between 12:00 and 16:00. Mice were habituated to the testing room for 1.5 h before the evaluation. Spontaneous locomotion was measured by open field testing under low lighting conditions. The total migration length for 3 min (10~190 sec after setting) in the test area (50 × 50 × 35 cm) was recorded. All data were analyzed by a video tracking system (LimeLight, Neuroscience Inc., Tokyo, Japan).

Immunohistochemistry. On the day following the last treatment of rotenone and EUE, mice were transcardially perfused with ice-cold saline followed by 4% paraformaldehyde (PFA) under deep pentobarbital

anesthesia. Brains and intestines were removed and post-fixed with 4% PFA for 24 h or 2 h, respectively, and soaked with 15% sucrose for cryoprotection. The brains and intestines were frozen with powdered dry ice and cut on a cryostat to make 20- μ m-thick brain and 14- μ m-thick intestinal sections. Brain coronal sections containing the mid-striatum (+0.6 to +1.0 mm from the bregma) and midbrain including the SNpc (-2.8 to -3.0 mm from the bregma) were collected.

Immunostaining of tyrosine hydroxylase (TH) was performed using slices at the level containing the SNpc. Brain slices were treated with 0.5% H₂O₂ for 30 min and then 1% normal goat serum for 30 min at room tem-

perature (RT). The slices were incubated with a rabbit anti-TH polyclonal antibody (diluted 1:1,000; Millipore, Temecula, CA, USA) diluted in 10-mM phosphate-buffered saline (PBS) containing 0.2% Triton X-100 (0.2% PBST) for 18 h at 4°C. After washing in 0.2% PBST (5×5 min), slices were incubated with biotinylated goat anti-rabbit IgG secondary antibody (1:1,000; Vector Laboratories, Inc., Burlingame, CA, USA) for 2 h at RT. After washing, slices were incubated with an avidin-biotin peroxidase complex (1:2,000) for 1 h at RT. TH-immunopositive signals were visualized by 3,3'-diaminobenzidine tetrahydrochloride, nickel ammonium sulfate and H₂O₂.

Double-immunostaining of α -Syn and TH was performed using nigral sections. The sections were pre-treated with 70% formic acid for 10 min at RT, and then incubated with 1% normal goat serum for 30 min at RT. Slices were reacted with a rabbit anti- α -Syn monoclonal antibody (1:1,000; Cell Signaling Technology, Inc., Danvers, MA, USA) and a mouse anti-TH monoclonal antibody (1:1,000; Millipore) for 18 h at 4°C. After washing in PBS, slices were incubated with Alexa Fluor 488-conjugated goat anti-rabbit IgG and Alexa Fluor 594-conjugated goat anti-mouse IgG secondary antibodies (1:1,000; Invitrogen, San Diego, CA, USA) for 2 h at RT. The slices were counterstained with Hoechst 33342 nuclear stain (10 μ g/ml) for 2 min.

Fluorescence immunohistochemistry of MT-1,2, glial fibrillary acidic protein (GFAP) or ionized calcium-binding adapter molecule 1 (Iba1) was performed on slices containing the striatum and SNpc. The sections were incubated with 1% normal goat or donkey serum for 30 min at RT, and then reacted with a rabbit anti-MT-1,2 polyclonal antibody (1:1,000; Frontier Institute, Hokkaido, Japan), a mouse anti-GFAP monoclonal antibody (1:10,000; Millipore) or a rabbit anti-Iba1 polyclonal antibody (1:500; Wako Pure Chemical Corporation, Osaka, Japan) for 18 h at 4°C. After washing, slices were incubated with Alexa Fluor 488-conjugated goat anti-rabbit IgG, Alexa Fluor 594-conjugated goat anti-mouse IgG or Alexa Fluor 488-conjugated donkey anti-rabbit IgG secondary antibodies (1:1,000; Invitrogen) for 2 h at RT, respectively.

To visualize the myenteric and submucosal plexus in the intestine, intestinal sections were pre-treated with 1% normal goat serum for 30 min at RT, and then reacted with a rabbit anti- β -tubulin III polyclonal antibody (1:1,000; Abcam, Danvers, MA, USA) for 18 h

at 4°C. After washing in PBS, slices were incubated with Alexa Fluor 488-conjugated goat anti-rabbit IgG antibody (1:1,000; Invitrogen) for 2 h at RT. Intestinal slices were finally counterstained with Hoechst 33342 nuclear stain.

All slides were analyzed under a fluorescence microscope (Olympus BX53, Tokyo, Japan) with cellSens imaging software (v1.16, Olympus) using a mercury lamp through 360-370 nm, 470-495 nm or 530-550 nm band-pass filters to excite Hoechst dye, Alexa Fluor 488 or Alexa Fluor 594, respectively. Colocalization of α -Syn and TH was confirmed by confocal laser-scanning microscopy (LSM780; Zeiss, Oberkochen, Germany). Light emitted from Hoechst 33342, Alexa Fluor 488 or Alexa Fluor 594 was collected through a 420-470 nm band-pass filter, a 500-550 nm band-pass filter, or a 570-640 nm band-pass filter, respectively. Images were taken and recorded using a ZEN software imaging system (Zeiss).

Quantification procedures. The numbers of TH-positive cells and α -Syn-positive dopaminergic neurons in the SNpc were counted under a microscope at magnifications of 100× and 400×, respectively. The numbers of MT- and GFAP-positive cells in the dorso-lateral striatum and SNpc were counted under a microscope at 200× magnification. The number and size of Iba1-positive cells in the striatum and SNpc were measured using NIH ImageJ (1.53c, NIH, Bethesda, MD, USA). The immunoreactivity of β -tubulin III in the intestine was analyzed under a microscope at 100× magnification and quantified using cellSens imaging software (Olympus). Integrated density was calculated as follows: integrated density=(signal density in the myenteric and submucosal plexus – background density) × area of positive signal in the plexus.

Statistical analyses. Data are expressed as means \pm SEMs. Repeated measures analysis of variance (ANOVA) was performed to evaluate time-dependent changes in body weight and behavioral parameters. To evaluate the results of immunostaining, one-way ANOVA was performed followed by a *post hoc* Tukey test. *P*-values < 0.05 were considered statistically significant.

Results

Effects of EUE administration on spontaneous locomotion in rotenone-induced PD model mice.

Rotenone treatment induced no weight loss at any time point. EUE administrations inhibited the age-dependent increase in body weight, especially in rotenone-injected mice (Fig.1B; group: $F(3,105)=33.404$, $p<0.001$; rotenone-water vs rotenone-EUE at 3 weeks and 4 weeks, $p<0.05$; time: $F(6,105)=18.936$, $p<0.001$; group \times time: $F(18,105)=0.606$, $p=0.888$). Total distance moved in the open field test was measured as an index of locomotor activity. The total distance was significantly decreased in rotenone-injected mice. EUE administrations showed a tendency to inhibit this decrease (Fig.1C; group: $F(3,70)=8.936$, $p<0.001$; time: $F(4,70)=1.490$, $p=0.214$; group \times time: $F(12,70)=0.404$, $p=0.957$).

Effects of EUE administration on dopaminergic neurodegeneration and microglial activation in the basal ganglia of rotenone-treated PD model mice. Rotenone treatment significantly decreased the number of TH-positive cells to approx. 65% of the vehicle-water control group in the SNpc ($F(3,43)=7.189$, $p<0.001$), and EUE administration almost completely prevented the rotenone-induced reduction of TH-positive cells (Fig.2A-C, $p<0.01$).

The number of Iba1-positive cells showed a tendency to increase in the striatum of rotenone-treated PD mice, but the increase did not reach statistical significance (Fig.2D, E; $F(3,38)=6.271$; vehicle-water vs rotenone-water, $p=0.076$). The size of Iba-1-positive cell bodies was significantly increased in the striatum by rotenone exposure (Fig.2F; $F(3,38)=20.825$, $p<0.001$), and the EUE administration prevented microglial activation (Fig.2F, $p<0.01$). In the SNpc, similar results were observed to those in the striatum (Fig.2G-I; number $F(3,37)=3.106$, $p<0.05$; size $F(3,37)=5.832$, $p<0.005$).

Effect of EUE administration on α -synuclein accumulation in dopaminergic neurons in the SNpc of rotenone-treated PD model mice. To examine α -Syn accumulation in the nigral dopaminergic neurons, we performed double immunostaining of TH and α -Syn. Rotenone treatment increased the α -Syn signals in the soma of TH-positive neurons in the SNpc (Fig.3A). In rotenone-treated mice, the number of TH-positive cells was decreased to approx. 63% of that of the control (Fig.3B, left; $F(3,29)=5.395$, $p<0.01$), corresponding with Fig.2, but the number of α -Syn- & TH-double positive cells was not changed (Fig.3B, middle; $F(3,29)=0.021$, $p=0.996$). To evaluate differences in the

number of TH-positive cells among groups, the ratio of the number of α -Syn- & TH-double positive cells to the number of TH-positive cells was calculated; the ratio was significantly higher in rotenone-injected mice (Fig.3B, right; $F(3,29)=3.373$, $p<0.05$), suggesting that α -Syn accumulated in the surviving dopaminergic neurons. EUE administrations inhibited the rotenone-induced α -Syn accumulation (Fig.3A, B).

Effects of EUE administration on MT-1, 2 expression in astrocytes in rotenone-treated PD model mice. To examine whether the EUE treatment up-regulated the anti-oxidative molecule MT in astrocytes, we performed double immunostaining of MT-1, 2 and GFAP using striatal and nigral sections. Interestingly, rotenone exposure significantly decreased the number of GFAP-positive astrocytes in the striatum (Fig.3C, D; $F(3,35)=4.541$, $p<0.01$) and SNpc (Fig.3E, F; $F(3,38)=3.169$, $p<0.05$). Accordingly, the numbers of MT- and GFAP-positive cells in rotenone-treated PD mice were decreased in the striatum (Fig.3D, middle; $F(3,35)=6.610$, $p<0.005$) and in the SNpc (Fig.3F, middle; $F(3,38)=6.143$, $p<0.005$). EUE administrations showed a tendency to inhibit the rotenone-induced reduction of GFAP-positive astrocytes (Fig.3D, left; $F(3,35)=4.541$, $p=0.549$ and 3F, left; $F(3,38)=3.169$, $p=0.222$) and significantly prevented the reduction of MT-expressing astrocytes (Fig.3D, middle; $F(3,35)=6.610$, $p<0.05$ and Fig.3F, middle; $F(3,38)=6.143$, $p<0.05$). The number of GFAP-positive astrocytes varies depending on the pathological condition. Therefore, we calculated the ratio of the number of MT- & GFAP-double positive cells to the number of GFAP-positive cells. Rotenone treatment was associated with a significant decrease of this ratio in both the striatum ($F(3,35)=9.572$, $p<0.01$) and SNpc ($F(3,38)=4.861$, $p<0.05$), which was completely prevented by EUE administration (Fig.3D, right, $p<0.01$ and Fig.3F, right, $p<0.05$).

Effects of EUE administration on the enteric plexus of rotenone-treated PD model mice. To examine the protective effects of EUE against rotenone-induced enteric neurodegeneration, we performed immunostaining of the neuronal marker β -tubulin III using intestinal sections (Fig.4A, B). Rotenone treatment decreased the β -tubulin III-positive areas of the myenteric and submucosal plexus (Fig.4A-C; $F(3,58)=4.093$, $p<0.05$) as well as the signal intensity for β -tubulin III (Fig.4D; $F(3,58)=3.660$, $p<0.05$).

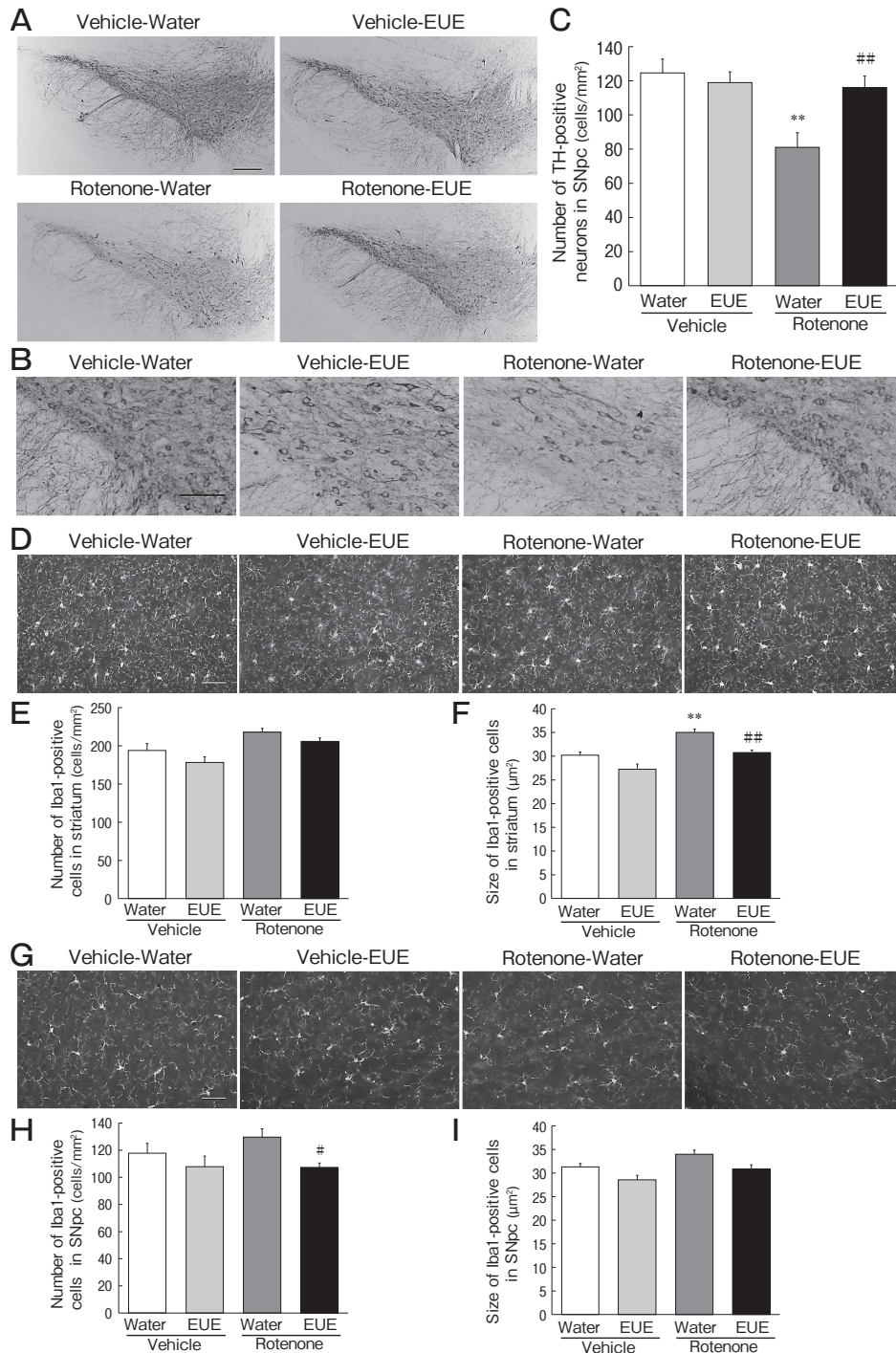


Fig. 2 Effects of EUE administrations on nigrostriatal dopaminergic neurodegeneration and microglial activation in the basal ganglia of rotenone-treated PD model mice. **A & B**, Representative photographs of immunohistochemistry for TH in the SNpc of a rotenone-treated mouse with EUE administration. Scale bar=200 μm (A), 100 μm (B); **C**, Changes in the number of TH-positive cells; **D & G**, Representative photographs of immunohistochemistry for Iba1 in the striatum (D) and SNpc (G) after 4-week rotenone with or without 5-week EUE treatment. Scale bar = 50 μm; **E & H**, The number of striatal (E) or nigral (H) Iba1-positive cells; **F & I**, The size of striatal (F) and nigral (I) Iba1-positive cells. Each value represents the mean ± SEM (n=4-6). ***p*<0.01 vs. Vehicle-Water group; #*p*<0.05; ##*p*<0.01 vs. Rotenone-Water group.

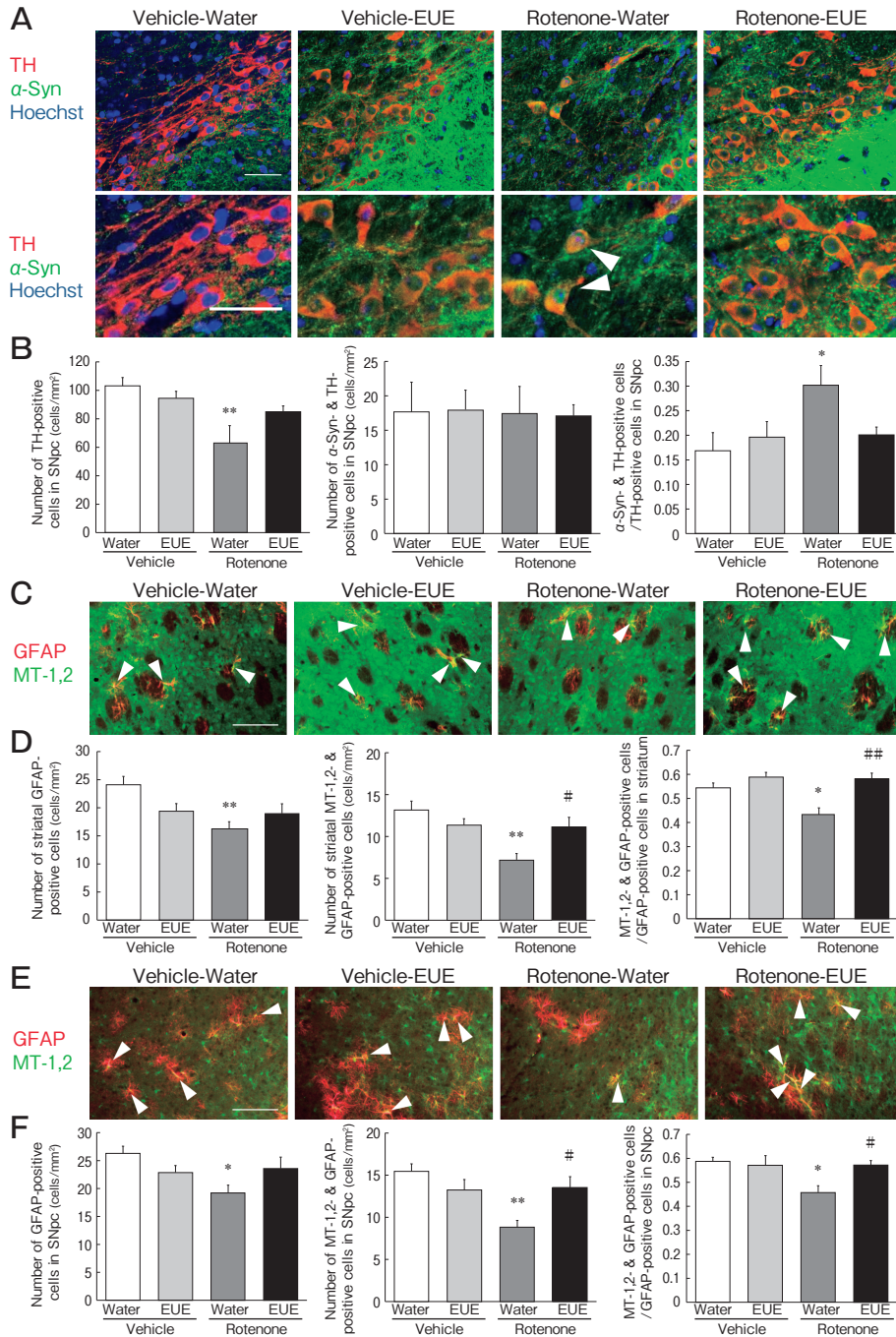


Fig. 3 Effect of EUE administration on α -Syn expression and MT-1,2 expression in the basal ganglia of rotenone-treated PD model mice. **A**, Representative photomicrographs of immunohistochemistry for TH (red) and α -Syn (green) in the SNpc of rotenone- and EUE-treated or -untreated mice. Blue: Hoechst 33342. Scale bar = 40 μ m; **B**, The number of TH-positive cells (left), the number of α -Syn- & TH-double positive cells (middle) and the ratio of the number of α -Syn- & TH-double positive cells to the number of TH-positive cells (right) in the SNpc; **C & E**, Representative photomicrographs of immunohistochemistry for GFAP (red) and MT-1,2 (green) in the striatum (C) and SNpc (E) after rotenone treatment with and without EUE treatment. Scale bar = 100 μ m; **D & F**, The number of GFAP-positive cells (left), the number of MT-1,2- & GFAP-double positive cells (middle) and the ratio of the number of MT-1,2- & GFAP-double positive cells to the number of GFAP-positive cells (right) in the striatum (D) and SNpc (F). Each value represents the mean \pm SEM (n = 4-6). * p < 0.05; ** p < 0.01 vs. Vehicle-Water group; # p < 0.05; ## p < 0.01 vs. Rotenone-Water group.

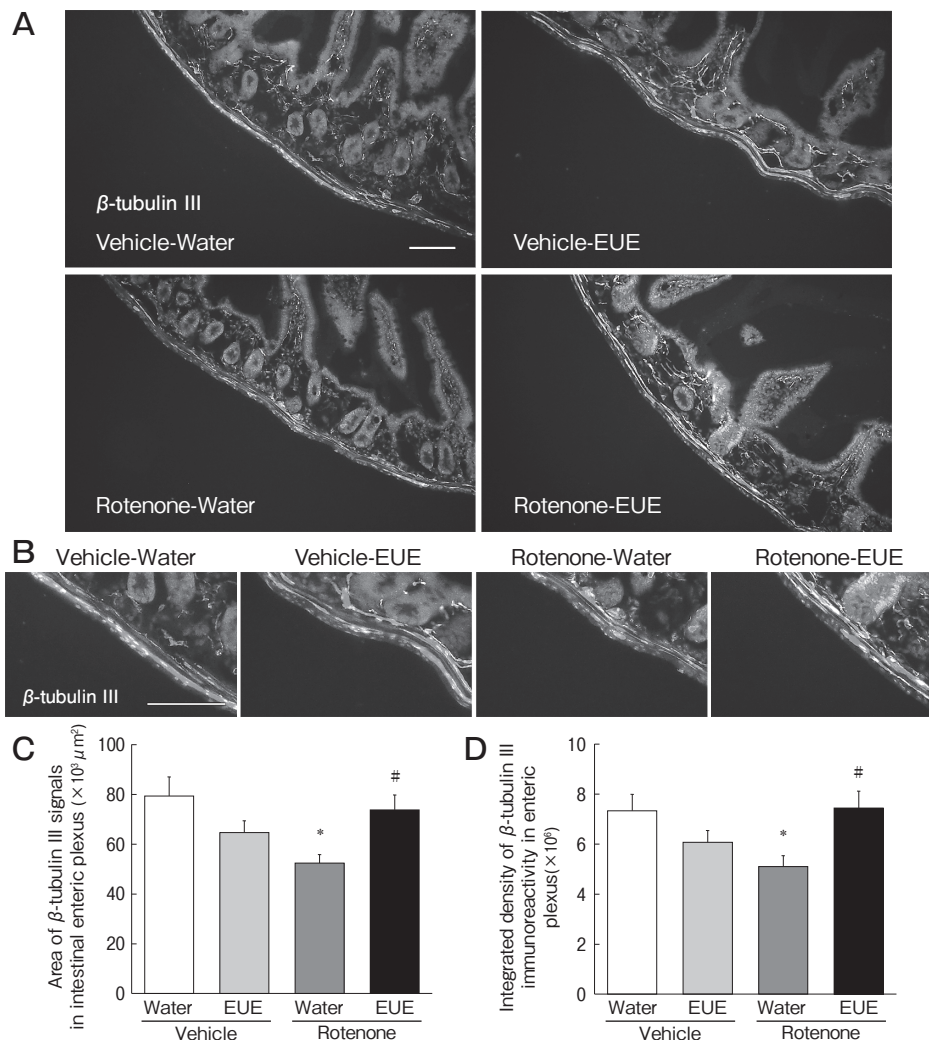


Fig. 4 Effects of EUE administrations on neurodegeneration in the myenteric plexus of rotenone-treated mice. **A**, Representative photographs of immunohistochemistry for β -tubulin III in the enteric plexus of rotenone-treated mice with and without EUE treatment; **B**, Photomicrographs of the area of β -tubulin III-positive myenteric plexus. Scale bar = 100 μm ; **C**, Area size of β -tubulin III-positive signals in enteric plexus; **D**, The integrated density of β -tubulin III immunoreactivity. Each value represents the mean \pm SEM ($n=4-6$). * $p<0.05$ vs. Vehicle-Water group, # $p<0.05$ vs. Rotenone-Water group.

EUE administration significantly prevented the decrease of area and signal intensity of neurons in the enteric plexus (Fig. 4C and 4D, $p<0.05$, respectively).

Discussion

In this study, we demonstrated the central and peripheral neuroprotective effects of EUE on rotenone-treated PD model mice. EUE administration also prevented rotenone-induced astrocyte dysfunction and activation of microglia. Furthermore, the treatment

restored motor dysfunction in rotenone-injected PD mice.

EU is a traditional herbal medicine which contains 112 secondary metabolites; in particular, chlorogenic acid and catechin are known to scavenge reactive oxygen species (ROS) directly and chelate metals such as Fe [31]. Previous studies have also reported the neuroprotective effects of EUE [26-28, 32]. EU inhibited nuclear translocation of nuclear factor- κB (NF- κB) and apoptosis induced by the neurotoxin 6-hydroxydopamine in SH-SY5Y neuroblastoma cells [32]. Also in SH-SY5Y

cells, EU ameliorated the dysfunction of the ubiquitin-proteasome system induced by another dopaminergic neurotoxin, 1-methyl-4-phenyl-1,2,3,6-tetrahydropyridine (MPTP) [27]. EU up-regulated autophagic factors to prevent dopaminergic neurodegeneration and motor dysfunction in MPTP-injected zebrafish [26]. Furthermore, EU administration suppressed the p38/c-Jun N-terminal kinase (JNK)-Fos-like 2 (Fosl2) pathway in MPTP-induced PD model mice [28]. Using the same low-dose rotenone-induced PD model mice as in this study, we previously showed the neuroprotective effects of treatment with chlorogenic acid, a component of EU, against dopaminergic neuronal loss in the SNpc [24]. In the present study, chronic EUE administration inhibited α -Syn accumulation in the nigral DA neurons of rotenone-exposed PD mice. The ubiquitin-proteasome system and autophagy are essential to the degradation of α -Syn [33]. Therefore, EUE may inhibit α -Syn accumulation by activation of a protein degradation system.

Astrocytes play an important role in neuroprotection by secretion of anti-oxidative molecules and removal of neurotoxic molecules, and astrocyte dysfunction is related to neurodegenerative diseases [16,34]. Activated astrocytes have been detected in various PD models [35,36]. In contrast, the number of GFAP-positive astrocytes was decreased in the brains of rotenone-treated mice in the present study. Furthermore, rotenone exposure decreased MT-1,2 expression in astrocytes. These results suggest that EUE prevented rotenone-induced astrocyte dysfunction and reduction of MT-1,2 expression. MT expression is regulated by nuclear factor erythroid 2-related factor 2 (Nrf2), metal regulatory transcription factor 1, glucocorticoids, and signal transducers and activators of transcription [21,37,38]. EU and aucubin, a compound of EUE, promoted nuclear translocation of Nrf2 and up-regulated transcription of downstream anti-oxidative molecules, such as heme oxygenase-1 and NAD(P)H quinone oxidoreductase-1 [39-41]. We previously demonstrated that astrocytes up-regulated MT-1,2 through nuclear translocation of Nrf2 in response to oxidative stress [20]. Taken together, these findings suggest that EUE may induce MT-1,2 expression in astrocytes by activation of the Nrf2 pathway.

Microglia contribute to neuroinflammation in the CNS. Various stimuli activate microglia to be transformed into hypertrophic cell bodies (amoeboid

microglia) and then to accumulate. Activated microglia release pro-inflammatory cytokines through activation of the NF- κ B pathway [34]. Such microglial activation is involved in dopaminergic degeneration in PD [13]. In the present experiment, EUE administration inhibited microglial activation in the brains of PD model mice. It was reported that EU inhibited the nuclear translocation of NF- κ B and the expression of pro-inflammatory cytokines induced by lipopolysaccharide [39]. These observations suggest that EUE exerts neuroprotective effects, not only by anti-oxidative properties, but also an anti-inflammatory effect, *i.e.*, the inhibition of microglial activation. However, it is hard to identify the active molecules in EUE that promote the neuroprotective effects, because EU contains so many components.

In this study, we also demonstrated the neuroprotective effects of EUE in the intestinal plexus of rotenone-injected mice. In the intestinal plexus, MT-1,2 is expressed in GFAP-positive glial cells. Our previous study demonstrated the neuroprotective effects of MT expression in enteric glial cells, because the rotenone-induced myenteric neurodegeneration was aggravated in MT-1,2-knockout mice [22]. In addition, coffee components, caffeic acid and chlorogenic acid, prevented the loss of neurons in the myenteric plexus of rotenone-treated PD models with up-regulating MT [24]. The induction of MT expression may be one of the initial molecular events in this myenteric neuroprotection. As mentioned above, chlorogenic acid, a major component of EUE, has demonstrated the ability to up-regulate MT [24]. Taken together with these observations, the present results suggested that EUE, probably chlorogenic acid, could exert neuroprotective effects by MT up-regulation in enteric glial cells.

Animals in this study received EUE (600 mg/kg/day) by daily oral administration. The dosage of EUE was higher than the daily drinking dosage (2,000 mg/day). Oral EU administrations of 150-5,000 mg/kg/day for 8 days have been shown to prevent dopaminergic neurodegeneration in MPTP-injected PD model mice [26,27]. To confirm the effect of EUE on MT expression, in a preliminary experiment we administered EUE (300 and 600 mg/kg/day, *p.o.*) to mice for 2 weeks and found that administration of EUE at 600 mg/kg/day up-regulated MT-1,2 expression in astrocytes (data not shown). These findings were the basis of the determination of the EUE dosage of 600 mg/kg/day in the

present study. Further examination will be required in order to clarify the neuroprotective effects of a lower dose of EUE by long-term administration.

As the EUE contained chlorogenic acid at 40.30 mg/g, the dosage of EUE (600 mg/kg/day) in the present study is equivalent to 24.18 mg/kg/day of chlorogenic acid. This is almost half the dose of chlorogenic acid (50 mg/kg/day for 4 weeks) used in our previous study [24], which showed similar neuroprotective effects against central and enteric neurodegeneration using the same rotenone-treated PD models. These data imply that either components of EUE other than chlorogenic acid also exert neuroprotective effects or that a dose of approx. 25 mg/kg/day of chlorogenic acid is sufficient for neuroprotection.

In conclusion, as well as neuroprotective effects of chlorogenic acid, a component of coffee, against neurodegeneration of nigral dopaminergic neurons and enteric neurons [24], EUE exerted central and peripheral neuroprotection and improvement of behavior dysfunction in rotenone-induced PD model mice, suggesting that EUE could be a neuroprotective supplemental agent for PD.

Acknowledgments. The authors thank all colleagues who contributed to this study. This work was funded by JSPS KAKENHI Grants for Scientific Research (C) (JP19K07993 to I.M., JP21K07415 to M.A.) and the grant from Japanese Society of Eucommia (to M.A.).

References

- Chaudhuri KR, Healy DG, Schapira AH and National Institute for Clinical E: Non-motor symptoms of Parkinson's disease: diagnosis and management. *Lancet Neurol* (2006) 5: 235–245.
- Fasano A, Visanji NP, Liu LW, Lang AE and Pfeiffer RF: Gastrointestinal dysfunction in Parkinson's disease. *Lancet Neurol* (2015) 14: 625–639.
- Braak H, Del Tredici K, Rüb U, de Vos RA, Jansen Steur EN and Braak E: Staging of brain pathology related to sporadic Parkinson's disease. *Neurobiol Aging* (2003) 24: 197–211.
- Braak H, de Vos RA, Bohl J and Del Tredici K: Gastric α -synuclein immunoreactive inclusions in Meissner's and Auerbach's plexuses in cases staged for Parkinson's disease-related brain pathology. *Neurosci Lett* (2006) 396: 67–72.
- Wakabayashi K, Takahashi H, Ohama E and Ikuta F: Parkinson's disease: an immunohistochemical study of Lewy body-containing neurons in the enteric nervous system. *Acta Neuropathol* (1990) 79: 581–583.
- Kim S, Kwon SH, Kam TI, Panicker N, Karuppagounder SS, Lee S, Lee JH, Kim WR, Kook M, Foss CA, Shen C, Lee H, Kulkarni S, Pasricha PJ, Lee G, Pomper MG, Dawson VL, Dawson TM and Ko HS: Transneuronal propagation of pathologic α -synuclein from the gut to the brain models Parkinson's disease. *Neuron* (2019) 103: e627–641.
- Borghammer P and Van Den Berge N: Brain-First versus Gut-First Parkinson's Disease: A Hypothesis. *J Parkinsons Dis* (2019) 9: S281–S295.
- Challis C, Hori A, Sampson TR, Yoo BB, Challis RC, Hamilton AM, Mazmanian SK, Volpicelli-Daley LA and Gradinaru V: Gut-seeded α -synuclein fibrils promote gut dysfunction and brain pathology specifically in aged mice. *Nat Neurosci* (2020) 23: 327–336.
- Klingelhoefer L and Reichmann H: Pathogenesis of Parkinson disease—the gut-brain axis and environmental factors. *Nat Rev Neurol* (2015) 11: 625–636.
- Perez-Pardo P, Kliet T, Dodiya HB, Broersen LM, Garssen J, Keshavarzian A and Kraneveld AD: The gut-brain axis in Parkinson's disease: Possibilities for food-based therapies. *Eur J Pharmacol* (2017) 817: 86–95.
- Svensson E, Horváth-Puhó E, Thomsen RW, Djurhuus JC, Pedersen L, Borghammer P and Sørensen HT: Vagotomy and subsequent risk of Parkinson's disease. *Annals of neurology* (2015) 78: 522–529.
- Van Den Berge N, Ferreira N, Mikkelsen TW, Alstrup AKO, Tamgüney G, Karlsson P, Terkelsen AJ, Nyengaard JR, Jensen PH and Borghammer P: Ageing promotes pathological alpha-synuclein propagation and autonomic dysfunction in wild-type rats. *Brain* (2021) 144: 1853–1868.
- Miyazaki I and Asanuma M: The rotenone models reproducing central and peripheral features of Parkinson's disease. *NeuroSci* (2020) 1: 1–14.
- Tanner CM, Kamel F, Ross GW, Hoppin JA, Goldman SM, Korell M, Marras C, Bhudhikanok GS, Kasten M, Chade AR, Comyns K, Richards MB, Meng C, Priestley B, Fernandez HH, Cambi F, Umbach DM, Blair A, Sandler DP and Langston JW: Rotenone, paraquat, and Parkinson's disease. *Environ Health Perspect* (2011) 119: 866–872.
- Miyazaki I, Isooka N, Imafuku F, Sun J, Kikuoka R, Furukawa C and Asanuma M: Chronic systemic exposure to low-dose rotenone induced central and peripheral neuropathology and motor deficits in mice: Reproducible animal model of Parkinson's disease. *Int J Mol Sci* (2020) 21: 3254.
- Booth HDE, Hirst WD and Wade-Martins R: The role of astrocyte dysfunction in Parkinson's disease pathogenesis. *Trends Neurosci* (2017) 40: 358–370.
- Pekny M, Pekna M, Messing A, Steinhäuser C, Lee JM, Pappas V, Hol EM, Sofroniew MV and Verkhratsky A: Astrocytes: a central element in neurological diseases. *Acta Neuropathol* (2016) 131: 323–345.
- Miyazaki I and Asanuma M: Therapeutic strategy of targeting astrocytes for neuroprotection in Parkinson's disease. *Curr Pharm Design* (2017) 23: 4936–4947.
- Miyazaki I and Asanuma M: Neuron-astrocyte interactions in Parkinson's disease. *Cells* (2020) 9: 2623.
- Miyazaki I, Asanuma M, Kikkawa Y, Takeshima M, Murakami S, Miyoshi K, Sogawa N and Kita T: Astrocyte-derived metallothionein protects dopaminergic neurons from dopamine quinone toxicity. *Glia* (2011) 59: 435–451.
- Ruttikay-Nedecky B, Nejdil L, Gumulec J, Zitka O, Masarik M, Eckschlager T, Stiborova M, Adam V and Kizek R: The role of metallothionein in oxidative stress. *Int J Mol Sci* (2013) 14: 6044–6066.
- Murakami S, Miyazaki I, Sogawa N, Miyoshi K and Asanuma M: Neuroprotective effects of metallothionein against rotenone-induced myenteric neurodegeneration in parkinsonian mice.

- Neurotox Res (2014) 26: 285–298.
23. Palmiter RD: The elusive function of metallothioneins. *Proc Natl Acad Sci USA* (1998) 95: 8428–8430.
 24. Miyazaki I, Isooka N, Wada K, Kikuoka R, Kitamura Y and Asanuma M: Effects of enteric environmental modification by coffee components on neurodegeneration in rotenone-treated mice. *Cells* (2019) 8: 221.
 25. He X, Wang J, Li M, Hao D, Yang Y, Zhang C, He R and Tao R: *Eucommia ulmoides* Oliv.: ethnopharmacology, phytochemistry and pharmacology of an important traditional Chinese medicine. *J Ethnopharmacol* (2014) 151: 78–92.
 26. Fan S, Yin Q, Li D, Ma J, Li L, Chai S, Guo H and Yang Z: Anti-neuroinflammatory effects of *Eucommia ulmoides* Oliv. in a Parkinson's mouse model through the regulation of p38/JNK-Fosl2 gene expression. *J Ethnopharmacol* (2020) 260: 113016.
 27. Guo H, Shi F, Li M, Liu Q, Yu B and Hu L: Neuroprotective effects of *Eucommia ulmoides* Oliv. and its bioactive constituent work via ameliorating the ubiquitin-proteasome system. *BMC Complement Altern Med* (2015) 15: 151.
 28. Zhang S, Yu Z, Xia J, Zhang X, Liu K, Sik A and Jin M: Anti-Parkinson's disease activity of phenolic acids from *Eucommia ulmoides* Oliver leaf extracts and their autophagy activation mechanism. *Food Funct* (2020) 11: 1425–1440.
 29. Hashikawa-Hobara N, Hashikawa N, Sugiman N, Hosoo S, Hirata T, Yamaguchi Y, Yamasaki H, Kawasaki H and Nishibe S: Oral administration of *Eucommia ulmoides* Oliv. leaves extract protects against atherosclerosis by improving macrophage function in ApoE knockout mice. *J Food Sci* (2020) 85: 4018–4024.
 30. Hosoo S, Koyama M, Kato M, Hirata T, Yamaguchi Y, Yamasaki H, Wada A, Wada K, Nishibe S and Nakamura K: The restorative effects of *Eucommia ulmoides* Oliver leaf extract on vascular function in spontaneously hypertensive rats. *Molecules* (2015) 20: 21971–21981.
 31. Zhou ZD, Xie SP, Saw WT, Ho PGH, Wang H, Lei Z, Yi Z and Tan EK: The therapeutic implications of tea polyphenols against dopamine (DA) neuron degeneration in Parkinson's disease (PD). *Cells* (2019) 8: 911.
 32. Kwon SH, Ma SX, Hong SI, Kim SY, Lee SY and Jang CG: *Eucommia ulmoides* Oliv. Bark. attenuates 6-hydroxydopamine-induced neuronal cell death through inhibition of oxidative stress in SH-SY5Y cells. *J Ethnopharmacol* (2014) 152: 173–182.
 33. Xilouri M, Brekk OR and Stefanis L: α -Synuclein and protein degradation systems: a reciprocal relationship. *Mol Neurobiol* (2013) 47: 537–551.
 34. Kwon HS and Koh SH: Neuroinflammation in neurodegenerative disorders: the roles of microglia and astrocytes. *Transl Neurodegener* (2020) 9: 42.
 35. Murakami S, Miyazaki I, Miyoshi K and Asanuma M: Long-term systemic exposure to rotenone induces central and peripheral pathology of Parkinson's disease in mice. *Neurochem Res* (2015) 40: 1165–1178.
 36. Su RJ, Zhen JL, Wang W, Zhang JL, Zheng Y and Wang XM: Time-course behavioral features are correlated with Parkinson's disease-associated pathology in a 6-hydroxydopamine hemiparkinsonian rat model. *Mol Med Rep* (2018) 17: 3356–3363.
 37. Miyazaki I and Asanuma M: Serotonin 1A receptors on astrocytes as a potential target for the treatment of Parkinson's disease. *Curr Med Chem* (2016) 23: 686–700.
 38. Shih AY, Johnson DA, Wong G, Kraft AD, Jiang L, Erb H, Johnson JA and Murphy TH: Coordinate regulation of glutathione biosynthesis and release by Nrf2-expressing glia potently protects neurons from oxidative stress. *J Neurosci* (2003) 23: 3394–3406.
 39. Kwon SH, Ma SX, Hwang JY, Ko YH, Seo JY, Lee BR, Lee SY and Jang CG: The anti-inflammatory activity of *Eucommia ulmoides* Oliv. Bark. involves NF- κ B suppression and Nrf2-dependent HO-1 induction in BV-2 microglial cells. *Biomol Ther (Seoul)* (2016) 24: 268–282.
 40. Shen B, Zhao C, Wang Y, Peng Y, Cheng J, Li Z, Wu L, Jin M and Feng H: Aucubin inhibited lipid accumulation and oxidative stress via Nrf2/HO-1 and AMPK signalling pathways. *J Cell Mol Med* (2019) 23: 4063–4075.
 41. Wang H, Zhou XM, Wu LY, Liu GJ, Xu WD, Zhang XS, Gao YY, Tao T, Zhou Y, Lu Y, Wang J, Deng CL, Zhuang Z, Hang CH and Li W: Aucubin alleviates oxidative stress and inflammation via Nrf2-mediated signaling activity in experimental traumatic brain injury. *J Neuroinflammation* (2020) 17: 188.